

# Evaluation of Soil Parameters from Piezocone Tests

KAARE SENNESET, ROLF SANDVEN, AND NILMAR JANBU

The interpretation and evaluation of soil parameters determined by cone penetration tests (CPTs) have been a part of our research program for the last 15 to 20 years. A theoretical framework has been established, and CPT results have been compared and calibrated to laboratory data for a wide variety of soils. The pore pressure measurements that enable us to find effective shear strength parameters, as well as settlement parameters (such as the coefficient of consolidation) have been especially useful. In general, piezocone penetration test data have proved to be very useful and valuable additions to sampling and laboratory investigations. In some soils, we believe that the in situ method provides us with better data because sampling and laboratory handling may give us disturbed samples and erroneous results. In this paper, our interpretation and evaluation of piezocone data are demonstrated for a medium-stiff, overconsolidated clay.

Cone penetration tests (CPTs) with measurement of cone resistance ( $q_c$ ) and sleeve friction ( $f_s$ ) during penetration have been used in Norway since the early 1950s. In the early 1970s, the first attempts were made to measure the pore pressures developed around conically shaped piezometers ( $I$ ). These tests clearly showed that large pore pressures could be developed during penetration of fine-grained clays and silts.

The introduction of the piezocone (2,3) in the mid-1970s provided new possibilities for the interpretation of soil parameters and the identification of soil type. In particular, the simultaneous measurement of cone resistance ( $q_c$ ) and pore pressure ( $u_T$ ) in a piezocone penetration test (CPTU) permits the interpretation of test results in terms of effective stresses.

At the Norwegian Institute of Technology (NTH), research on the interpretation of piezocone test results has concentrated on the development of rational interpretation methods based on well-known theoretical principles. The methods have been applied to test records from various soil types, and systematic correlations have been made between laboratory reference parameters and interpreted values from CPTU data.

In this paper, the interpretation methods are demonstrated for Glava clay from the Trondheim region. This is a medium-stiff, overconsolidated clay of medium to low sensitivity. The following parameters have been interpreted and evaluated:

## Soil strength parameters:

- Undrained shear strength ( $s_u$ ), and
- Effective shear strength parameters [attraction ( $a$ ) and friction ( $\tan \phi'$ )];

## Deformation parameters:

- Compression moduli ( $M_i$  and  $M_n$ ),
- Stress history, preconsolidation pressure ( $\sigma'_c$ ), and
- Coefficient of consolidation ( $c_v$ ).

A classification chart that may aid in the classification of soil type on the basis of CPTU recordings is also presented.

## CPTU MEASUREMENTS AND CORRECTIONS

In a piezocone penetration test, the following recordings are usually made:

- Cone resistance ( $q_c$ ),
- Total pore pressure ( $u_T$ ) at reference location (Figure 1), and
- Sleeve friction ( $f_s$ ).

The terminology and symbols used in a CPTU are summarized in Figure 2. When the cone is subjected to water pressure on all sides, a shift in zero values will usually be recorded both for friction and cone resistance readings (4). The reason for this effect can be seen in Figure 1: the water pressures act on the end areas of the conical part and the friction sleeve, respectively, due to the jointed design of the cone. For most types of cones in practical use, these end areas are not equal in size, and an unbalanced force will occur during penetration. Therefore the recorded cone resistance  $q_c$  will be smaller than the true value, and the sleeve friction will be larger. To account for these effects, certain corrections should be applied to the original recordings (4,5). Equation 1 shows the correction to be applied to cone resistance:

$$q_T = q_c + (1 - a) \cdot u_T \quad (1)$$

where

- $q_T$  = corrected total cone resistance,
- $a$  = net area ratio ( $A_n/A_q < 1$ ) (Figure 1), and
- $u_T$  = total pore pressure at reference level (Figure 1).

Equation 2 shows the correction to be applied to sleeve friction:

$$f_T = f_s - (1 - k_s b) \cdot c \cdot u_T \quad (2)$$

where

- $f_T$  = corrected sleeve friction,

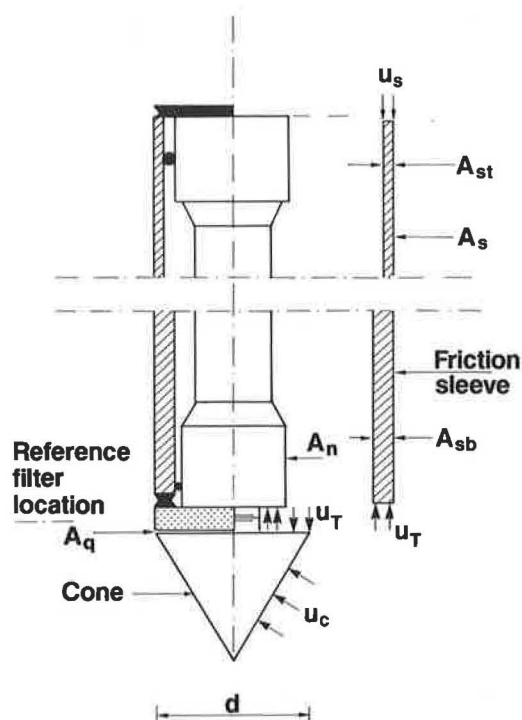


FIGURE 1 Correction of measured cone resistance for pore pressure effects.

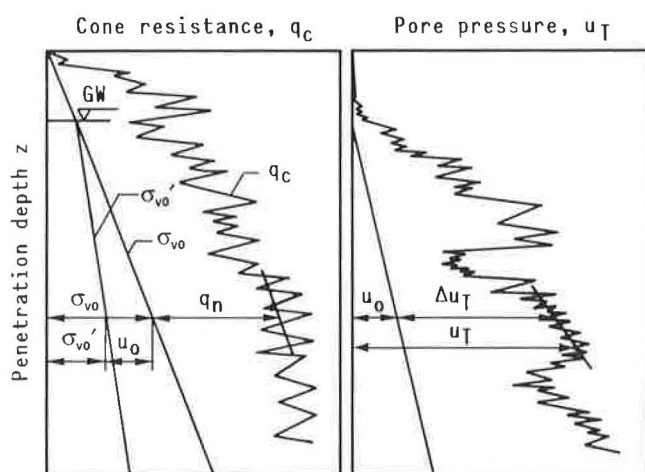


FIGURE 2 CPTU measurements and notations.

$b$  = sleeve end area ratio ( $A_{st}/A_{sb} < 1$ ) (Figure 1),  
 $c$  = sleeve area ratio ( $A_{sb}/A_s < 1$ ) (Figure 1),  
 $u_T$  = total pore pressure at reference filter location, and  
 $k_s = u_s/u_T \approx 0.6$  to  $0.8$  in soft clays.

These corrections may be important in soft clays and silts, where large pore pressures are generated during penetration. In coarse soils, the corrections are practically negligible because almost drained conditions prevail in the surrounding soil. To interpret the cone penetration process in terms of effective stresses, the pore pressures must be measured somewhere on or in the vicinity of the conical part. Two different locations have frequently been used for the pore pressure element:

- On the conical part, either at the tip or at mid-height of the cone,
- On the cylindrical part, immediately behind the cone neck. (This location has been recommended in a proposal to the International Society for Soil Mechanics and Foundation Engineering (6). It is referred to in this paper as the reference filter location.)

No specific filter location provides optimal pore pressure measurements for all practical applications. Unfortunately, the relative magnitude of the penetration pore pressure depends on where on the cone it is measured. Generally, the largest pore pressure is generated in the compression zone beneath the cone, whereas significantly lower pore pressure may be developed along the cylindrical part. Several researchers (7,8) have indicated that pore pressure behind the cone may be empirically related to pore pressure measured at the conical part.

The following expression may be used to adjust the pore pressure measured on the cone to make it correspond to the reference value (9):

$$u_T = u_0 + k(u_c - u_0) \quad (3)$$

where

$u_0$  = hydrostatic or initial in situ pore pressure,

$u_c$  = measured total pore pressure, and

$k$  = adjustment factor.

The adjustment factor  $k$  is primarily a function of soil type, soil properties, and the exact filter location on the cone. Experience from penetration tests in various soil types using cones with different filter locations is summarized in Table 1.

In some heavily overconsolidated clays and in very dense sands, negative pore pressures may exist at the reference level although positive pore pressures are measured on the cone. In such materials, negative values of  $k$  should be selected.

#### SITE AND LABORATORY INVESTIGATIONS—GLAVA CLAY

Interpretation of CPTU records from the medium-stiff, overconsolidated marine Glava clay has been selected for this paper. The clay is homogeneous, but some silt lenses are present in the upper parts of the profile. The clay is dry crusted down to about 1.5 m. Results from index tests and special tests in the laboratory are presented in Figure 3. The ground-

TABLE 1 EMPIRICAL VALUES OF  $k$  FOR ADJUSTMENT OF PORE PRESSURES

Soil Type	Filter Location	
	Cone Face, Mid-Height	Cone Tip
Normally consolidated clay	0.6–0.8	0.7–0.9
Slightly overconsolidated, sensitive clays	0.5–0.7	0.6–0.8
Heavily overconsolidated clays	0–0.3	0.1–0.3
Loose, compressible silts	0.5–0.6	0.5–0.7
Dilatant, dense silts	0–0.2	0.1–0.3
Loose, silty sands	0.2–0.4	0.5–0.6

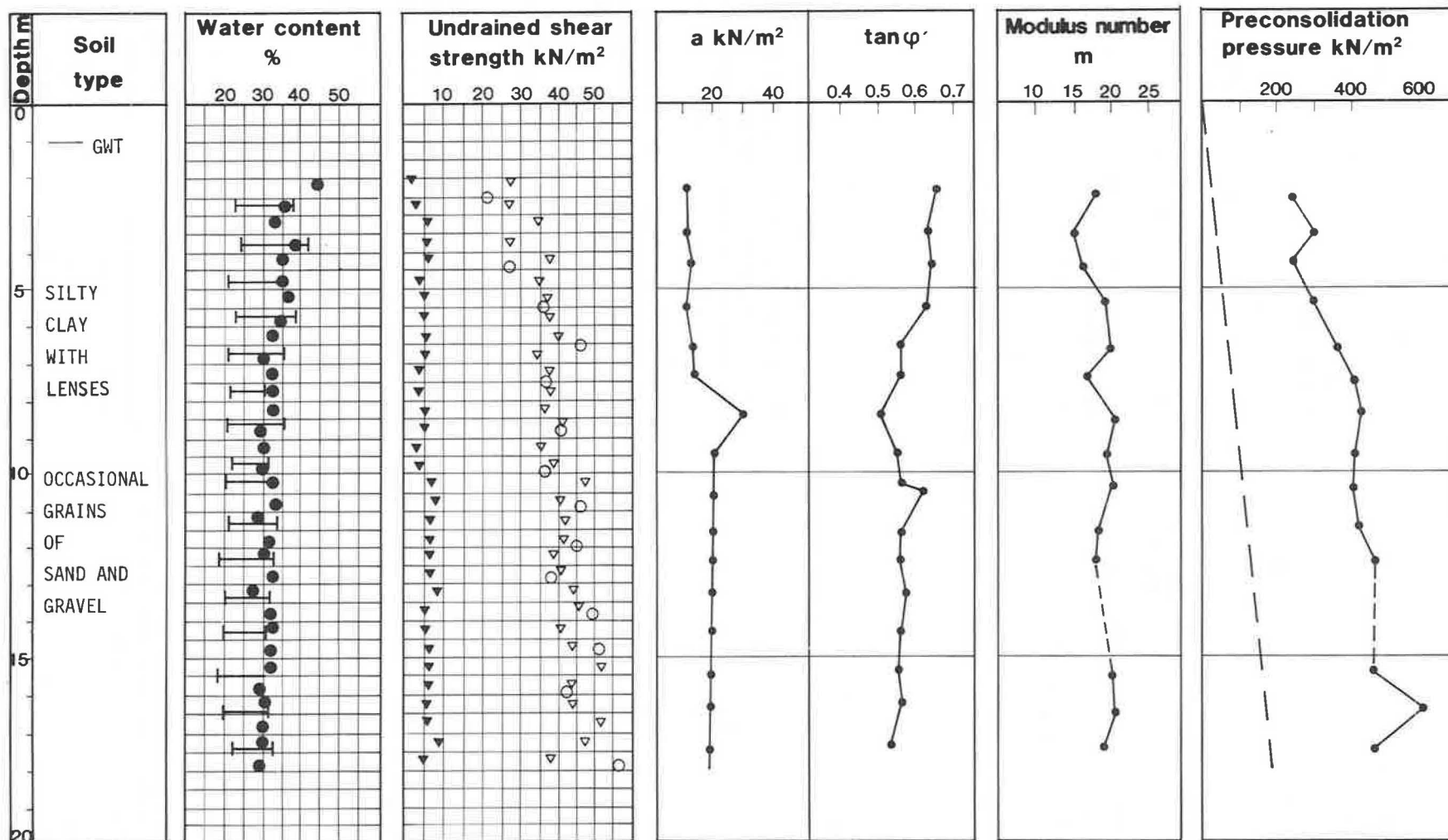


FIGURE 3 Soil profile for Glava clay.

water table is located at a depth of 1.0 m, and the initial pore pressure distribution ( $u_0$ ) is hydrostatic.

The laboratory testing program was performed on undisturbed clay samples obtained with the Geonor Ø 54 mm piston sampler. It included conventional index tests, CIU triaxial compression tests, and continuous-loading oedometer tests. The aim of this test program was to establish reference strength and deformation parameters for comparison with in situ parameters interpreted from the CPTU records.

The site investigations included three cone penetration tests with pore pressure measurements. A 10-cm<sup>2</sup>/60-degree piezocone with the filter at the reference location immediately behind the cone was used for all tests. Typical records of corrected cone resistance  $q_T$  and reference pore pressure  $u_T$  are shown in Figure 4.

The most important aspect of piezocone testing is the saturation of the pore pressure transducer system. Insufficient saturation may cause a delayed response to rapid changes in the pore pressure. The following procedure produced good results in Glava clay:

1. Saturation of filters before field work by (a) applying vacuum on submerged filters and (b) flushing with de-aired water; and
2. Preparation for field use by (a) applying high vacuum on the dismantled cone at the site for approximately 1 hour, (b) performing final cone assembly with the cone and filter submerged in de-aired water, and (c) sealing the filter with a rubber membrane before lowering the penetrometer down to the water level in a predrilled hole.

## SOIL STRENGTH

The cone penetration process involves many aspects of soil behavior that may complicate the development of a realistic analytical interpretation model. For example,

- Stresses and pore pressures around the cone vary in both vertical and radial directions;
- Singularities, high stress gradients, and high pore pressure gradients are present because of the cone geometry;

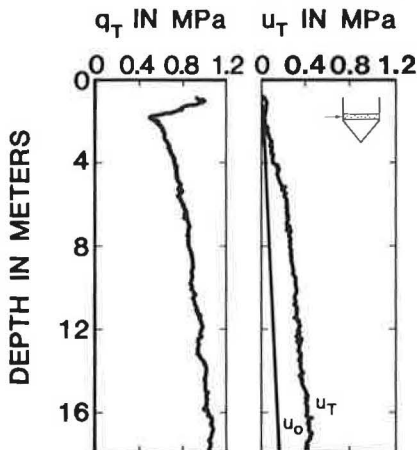


FIGURE 4 CPTU records for Glava clay.

- The geometrical shape and extent of plastified zones at failure are unknown; and

- The penetration takes place continuously, and large strains are imposed on the surrounding soil.

Considering these aspects, one may easily realize that a closed-form analytical solution to the cone penetration problem may be difficult to conceive. Analytical models from CPTU data for penetration of soil hence include simplifying assumptions and approximations that should be considered when evaluating interpreted parameters.

## Undrained Shear Strength

The undrained shear strength ( $s_u$ ) may be estimated from the cone data by using a theoretical relationship of the following form (10):

$$s_u = \frac{q_T - \sigma}{N_c} \quad (4)$$

where

$q_T$  = total corrected cone resistance,

$N_c$  = bearing capacity factor, and

$\sigma$  = in situ stress [either vertical overburden pressure ( $\sigma_{v0}$ ), horizontal pressure ( $\sigma_{h0} = K_0 \sigma_{v0}$ ), or octahedral pressure ( $\sigma_{oct} = 1/3(\sigma_{v0} + 2\sigma_{h0})$ )].

Various theoretical approaches have been introduced to determine the bearing capacity factor  $N_c$ ; these include bearing capacity theory (11,12), cavity expansion methods (13,14) and numerical approaches using linear or nonlinear soil models (15,16). However, a generally accepted theoretical model for determination of  $s_u$  has not yet been developed. Hence the interpretation of  $s_u$  is usually estimated from empirical relationships (17) such as

$$s_u = \frac{q_T - \sigma_{v0}}{N_{kT}} \quad (5)$$

where  $N_{kT}$  denotes a cone factor, including shape and depth factors.

The cone factor  $N_{kT}$  is usually determined from a reference value for  $s_u$ , either from a field vane test or a laboratory triaxial compression test. Values for  $N_{kT}$  seem to range from 10 to 15 for normally consolidated clays, and from about 15 to 19 for overconsolidated clays. Empirical values of  $N_{kT}$  are usually higher than the values of  $N_c$  obtained by theoretical models.

The large scatter in values of  $N_{kT}$  often limits the ability to produce a successful interpretation of  $s_u$  from CPTU data. Local correlations at the site are hence usually recommended, which, in fact, is not a very consistent procedure. Many reasons for the reported scatter may be relevant to mention; for example,

- The undrained shear strength is not a unique measure of the soil strength;
- The obtained value depends on the type of test performed;

- The obtained value of  $s_u$  is strain rate dependent; and
- The reference  $s_u$  for many empirical methods has been different.

The latter point may be discussed in further detail. It is well known that the maximum shear stress obtained in a clay sample subjected to triaxial compression depends on the consolidation stress level. Usually the samples are consolidated to the present in situ stress level, where the at-rest coefficient  $K_0$  is anticipated or approximated from empirical relationships. Overconsolidated soils were previously consolidated at higher stresses than those acting on the deposit today. These stress conditions may also be simulated in the consolidation phase for a triaxial test sample.

In Figure 5, a principal graph for the peak shear stress as a function of the consolidation stress  $\sigma'_{3c}$  is shown for Glava clay. The band reveals quite interesting tendencies:

- A large scatter is seen in the maximum shear stress ( $\tau_{max}$ ) for samples consolidated to the present in situ overburden pressure.
- Samples consolidated to or past the overconsolidation pressure indicate that there exists an upper limit of the maximum obtainable shear stress in the clay. This limit will correspond to the undrained shear strength  $s_u$ .

For Glava clay, values of  $N_{kT}$  based on  $\tau_{max}$  values from  $\sigma'_{3c}$ -consolidated test samples range from about 12 to 18. If the average peak shear stress from  $\sigma'_c$ -consolidated samples is utilized, the corresponding range becomes about 7 to 10. These empirically based values are in better agreement with reported theoretical values of the bearing capacity factor  $N_c$ .

Further research will be carried out in other types of clay to evaluate whether this approach has general applicability. If so, it may help narrowing the scatter in  $N_{kT}$  values and may perhaps explain the often-reported discrepancies between theoretical and empirical values.

### Effective Shear Strength

The effective shear strength parameters, friction ( $\tan \phi'$ ) and attraction ( $a$ ), over a stress range  $\Delta\sigma'$  are defined by the Mohr-

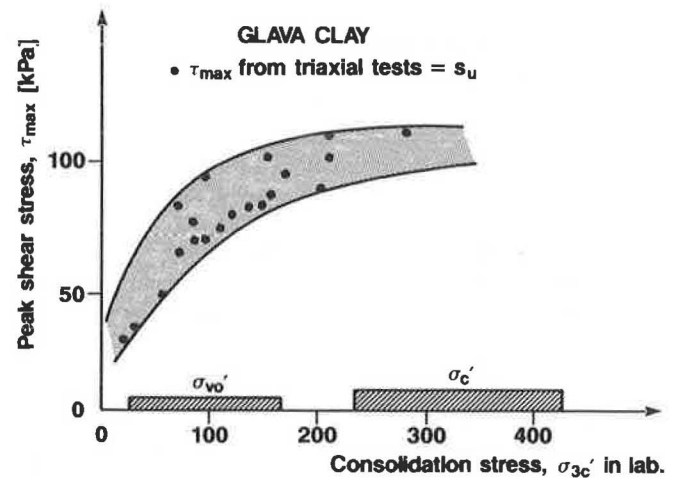


FIGURE 5 Principal graph of peak shear stress ( $\tau_{max}$ ) versus consolidation stress  $\sigma'_{3c}$  for Glava clay.

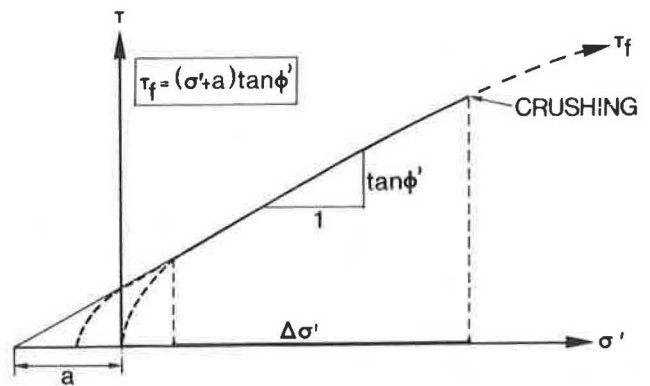


FIGURE 6 Definition of strength parameters in the Mohr-Coulomb criterion.

Coulomb failure criterion in Figure 6. Over a given range of working stresses, the strength envelope may best be approximated by the expression

$$\tau_f = (\sigma' + a) \tan \phi' \quad (6)$$

where  $\tau_f$  denotes shear strength, and  $\sigma'$  denotes effective normal

TABLE 2 TYPICAL VALUES OF ATTRACTION ( $a$ ) AND FRICTION ( $\tan \phi'$ ) (18)

	Shear Strength Parameters				
	$a$ (kPa)	$\tan \phi'$	$\phi'$	$N_m$	$B_q$
Clay					
Soft	5–10	0.35–0.45	19–24	1–3	0.8–1.0
Medium	10–20	0.40–0.55	19–29	3–5	0.6–0.8
Stiff	20–50	0.50–0.60	27–31	5–8	0.3–0.6
Silt					
Soft	0–5	0.50–0.60	27–31		
Medium	5–15	0.55–0.65	29–33	5–30	0–0.4
Stiff	15–30	0.60–0.70	31–35		
Sand					
Loose	0	0.55–0.65	29–33		
Medium	10–20	0.60–0.75	31–37	30–100	<0.1
Dense	20–50	0.70–0.90	35–42		
Hard, stiff soil, OC, cemented	>50	0.8–1.0	38–45	100	<0



stress on the failure plane. The term attraction ( $a$ ) is interpreted from the design stress range as the negative intercept of the normal stress axis ( $\sigma'$ ). The classical term cohesion ( $c$ ) is related to the attraction by the expression:

$$c = a \cdot \tan \phi' \quad (7)$$

Typical ranges of the shear strength parameters for some common soil types are given (18) in Table 2. The table may be useful for evaluating the parameter values interpreted from CPTU data.

It is important to note that a large silt content may increase the parameter values for clays but may reduce the parameter values in sands for otherwise similar conditions. Moreover, the presence of active clay minerals such as smectite and montmorillonite will decrease friction below the values given in Table 2.

### Theoretical Framework

The framework for effective stress interpretation has been the conventional bearing capacity approach based on the theory of plasticity. In the case of cone penetration in well-draining soils, which allow no excess pore pressure buildup in the soil, the formula for plane strain bearing capacity may be written (19) as

$$q_T + a = N_q(\sigma'_{v0} + a) \quad (8)$$

where

$\sigma'_{v0}$  = effective overburden pressure (at reference location),  
 $N_q$  = theoretical bearing capacity factor, and  
 $a$  = attraction.

In fine-grained soils, excess pore pressures will be generated around the cone and will decrease the ultimate bearing capacity. This is accounted for in the expression below (19):

$$q_n = (N_q - 1)(\sigma'_{v0} + a) - N_u \Delta u_T \quad (9)$$

where

$q_n = q_T - \sigma_{v0}$  = net cone resistance,  
 $\Delta u_T$  = excess pore pressure at reference location, and  
 $N_u$  = theoretical bearing capacity factor.

When the excess pore pressure is measured in the test, one can insert (19)

$$\Delta u_T = B_q q_n \quad (10)$$

[where  $B_q$  denotes pore pressure ratio ( $\Delta u_T/q_n$ )] into Equation 9 and obtain

$$q_n = N_m(\sigma'_{v0} + a) \quad (11)$$

where  $N_m = (N_q - 1)/(1 + N_u B_q)$ .

For the drained case,  $B_q = 0$ , and Equation 11 becomes similar to Equation 8.

The expression for the bearing capacity factor  $N_q$  may be written in the following way (18):

$$N_q = N_f \exp[(\pi - 2\beta) \tan \phi'] \quad (12)$$

where  $N_f$  equals  $\tan^2(45 + \frac{1}{2}\phi')$ , and  $\beta$  is the angle of plastification.

Figure 7 shows values of  $N_q$  as a function of  $\phi'$  and  $\beta$ , including an "empirical graph" for  $\beta$  based on various in situ strength tests in sands and silts. The band is extrapolated to cover clays. A definition of the angle of plastification ( $\beta$ ) in the idealized geometrical failure pattern is also included in Figure 7.

A theoretical solution of the bearing capacity factor  $N_u$  as a function of soil friction ( $\tan \phi'$ ) and base roughness ( $r$ ) has recently been developed at NTH (20). In the typical range of friction values in clays and silts where the term  $N_u \Delta u_T$  is significant, i.e., when  $\tan \phi'$  is in the range 0.3 to 0.7, the theoretical solution may be reasonably well approximated (19) by

$$N_u \sim 6 \tan \phi' (1 + \tan \phi') \quad (13)$$

The plane strain bearing capacity solution is hence primarily a function of the soil friction ( $\tan \phi'$ ) and the angle of plastification ( $\beta$ ).

### Soil classification

An impression of soil type may be gained from recorded values in a CPTU. If one uses the dimensionless parameters  $N_m = q_n/(\sigma'_{v0} + a)$  and  $B_q = \Delta u_T/q_n$ , the possible type of soil may be identified by using Table 2 (18).

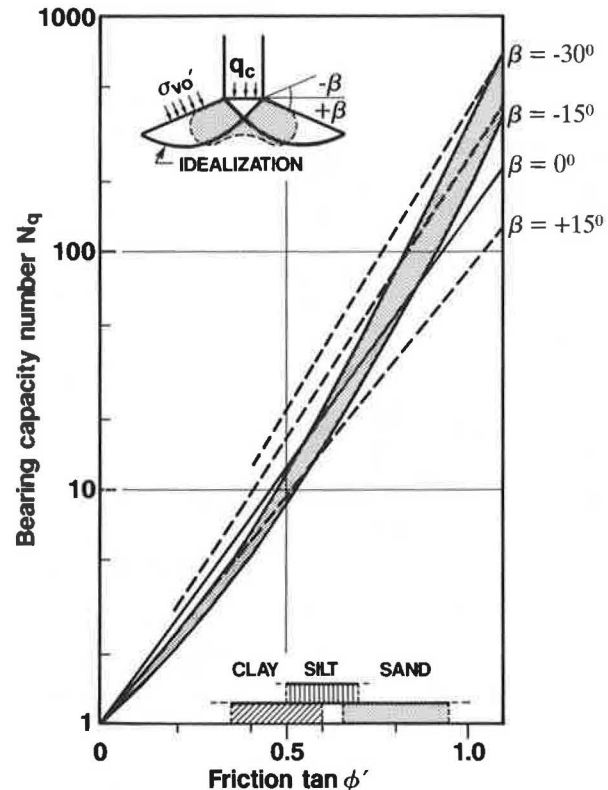


FIGURE 7 The bearing capacity factor  $N_q$ .

The modified classification chart shown in Figure 8, which is based on values of  $q_T$  and  $B_q$ , may be used for the same purpose (18). One should note that the values of  $B_q$  should be developed from the reference pore pressures measured immediately behind the cone, and that the corrected cone resistance  $q_T$  should be utilized in the classifications. The chart in Figure 8 may also be used when negative pore pressures are recorded at the reference location. The information on soil type and penetration conditions obtained from the classification may be valuable for the interpretation of strength parameters described later in this section.

#### Interpretation Method—Friction

The interpretation procedure is based on the following CPTU data:

- Corrected cone resistance ( $q_T$ ), and
- Excess pore pressure at reference location ( $\Delta u_T$ ).

Moreover, the following initial stress conditions in the penetrated soil must be known:

- Total overburden pressure ( $\sigma_{v0}$ ),
- Initial pore pressure distribution ( $u_0$ ), and
- Effective overburden pressure ( $\sigma'_{v0} = \sigma_{v0} - u_0$ ).

The following dimensionless parameters can then be found directly from the CPTU recordings: (a) the cone resistance number ( $N_m$ ):

$$N_m = \frac{q_T - \sigma_{v0}}{\sigma'_{v0} + a} = \frac{q_n}{\sigma'_{v0} + a} = \frac{N_q - 1}{1 + N_u B_q} \quad (14)$$

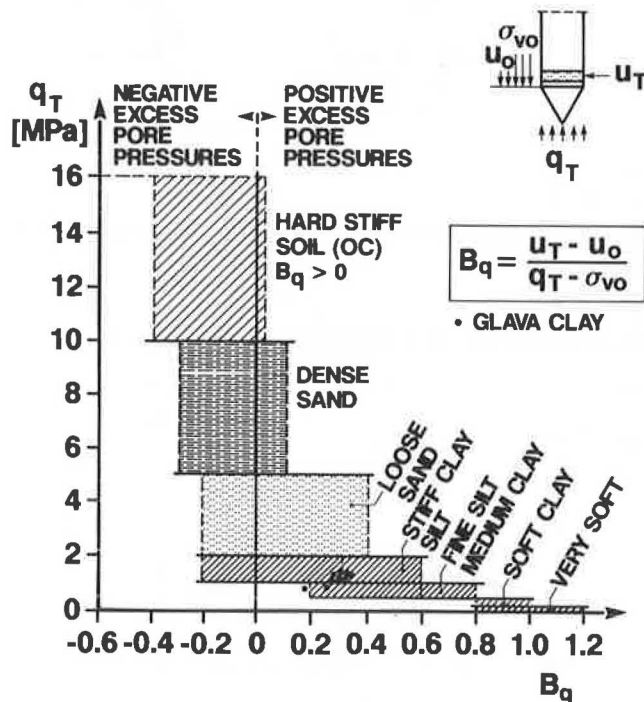


FIGURE 8 Chart for classification of soil type on the basis of CPTU recordings.

and (b) the pore pressure ratio ( $B_q$ ):

$$B_q = \frac{u_T - u_0}{\sigma'_{v0} + a} = \frac{\Delta u_T}{q_n} \quad (15)$$

The choice was made to derive values of  $B_q$  from the pore pressures measured on the reference filter location. The attraction values in Equation 14 may be evaluated theoretically or chosen on the basis of information on soil type and soil conditions.

The friction ( $\tan \phi'$ ) is then found from an interpretation chart, as shown in Figure 9. Because the interpreted value depends on the angle of plastification, several charts have to be developed in order to cover a range of possible values of  $\beta$ . In the example shown in Figure 9a,  $\tan \phi' = 0.66$  is determined from  $N_m = 12$  and  $B_q = 0.2$ . The interpretation procedure is, however, well suited for computer-assisted interpretation and presentation of results, and a computer program has been developed for the purpose (21).

#### Angle of Plastification

The angle of plastification ( $\beta$ ) expresses an idealized geometry of the generated failure zones around the advancing cone. This idealization requires that cone penetration be simulated as a quasistatic process. The value of  $\beta$  is hence difficult to assess, both experimentally and theoretically. However, it is reasonable to believe that  $\beta$  depends on soil properties such as compressibility and stress history, plasticity, and sensitivity. The easiest way to estimate typical values of  $\beta$  in various soils is to perform correlations between laboratory-determined  $\tan \phi'$  and interpreted values from CPTU. Results from such studies in various soil types performed at NTH over the recent years are summarized in Table 3. Information on soil type and soil conditions may be gained from the previously shown classification chart and table.

#### Attraction

Attraction ( $a$ ) may be estimated directly from the CPTU records, both for drained and undrained penetration (1,18). The suggested methods are applicable when relatively homogeneous soil deposits or layers are penetrated. In cases where such estimates cannot be obtained, it is suggested that typical values from triaxial tests on similar soils be used (9) (Table 2).

In CPTU interpretations, one may often obtain larger values than are usually found by triaxial testing. This may be due to sample disturbance of suction in the pores. However,

TABLE 3 TENTATIVE VALUES OF THE ANGLE OF PLASTIFICATION  $\beta$  IN VARIOUS SOIL TYPES (9)

Soil Type	Tentative Values of $\beta$ (degrees)
Dense sands, overconsolidated silts, high plastic clays, low-compressible overconsolidated clays	-20 to -10
Medium sands and silts, sensitive clays, high-compressible clays	-5 to +5
Loose silts, clayey silts	+10 to +20

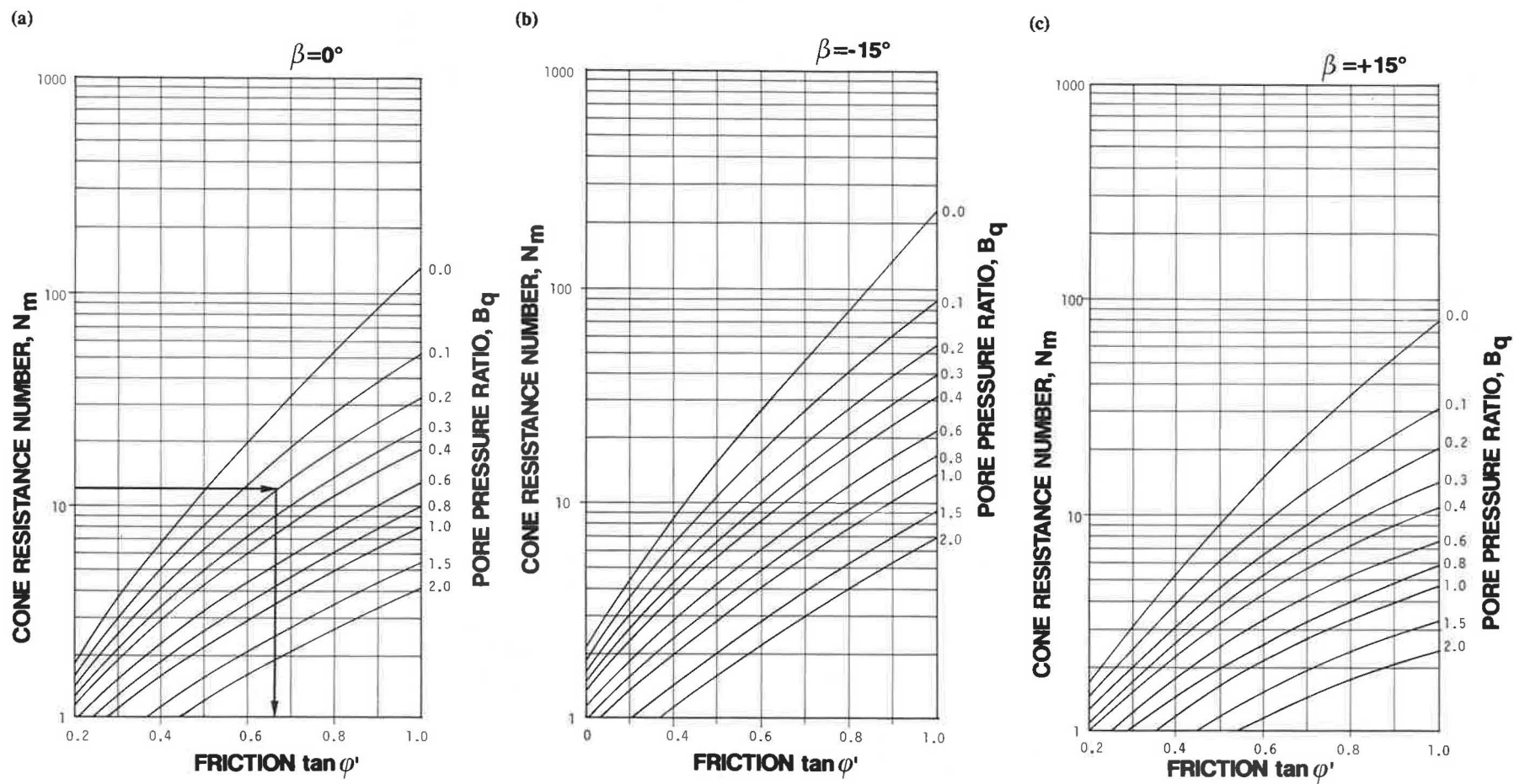


FIGURE 9 (a) Interpretation diagram for  $\beta = 0$  degrees; (b) interpretation diagram for  $\beta = -15$  degrees; (c) interpretation diagram for  $\beta = +15$  degrees.



uncertainties in the determination of attraction have only small effects on interpreted friction at greater penetration depths ( $z > 10$  m).

### Results for Glava Clay

In Figure 10, values of  $\tan \phi'$  interpreted from CPTU are compared to reference values obtained from triaxial compression tests. In the upper 10 m of the profile,  $\beta = -15$  degrees provided the best correspondance to the reference values, whereas  $\beta \sim 0$  degrees was appropriate below this depth. Attraction values determined from triaxial tests were used in the interpretation. Similar values of  $\beta$  have been found for other overconsolidated clays as well (9).

Further research will be carried out in order to gain more confidence in the selection of  $\beta$  values in various soils.

### SOIL DEFORMATION PARAMETERS

The penetration of a cone imposes large strains in the surrounding soil, and the distribution of stresses and pore pressures are complex and difficult to predict. This is in contradiction to real design problems, where relatively small strains are developed and a reasonable prediction of the effective stresses may be obtained. Hence, predictions of deformation moduli from CPTU data are usually based on empirical or semiempirical relationships.

The introduction of the piezocone made it possible to include pore pressure dissipation tests in situ. Much attention has been devoted to interpreting the results of such tests in order to estimate flow and consolidation characteristics of the soil.

In this section, simple methods of approximating soil deformation and consolidation parameters from CPTU data are presented and demonstrated for Glava clay. It should be stressed

that the methods are aiming only at a rough estimate of the parameter values. Laboratory tests should be carried out in order to establish design values of the deformation parameters for clays.

### Compression Moduli

The compressibility of the soil may conveniently be expressed by the tangent modulus ( $M$ ) (22), where

$$M = d\sigma'/d\epsilon \quad (16)$$

The tangent modulus varies with the effective stress  $\sigma'$  in different ways for various soil types. It has been found that all types of variations may be described by the following general expression (22):

$$M = m \cdot \sigma_a \cdot \left( \frac{\sigma'}{\sigma_a} \right)^{1-a} \quad (17)$$

where

- $m$  = modulus number,
- $\sigma_a$  = reference stress ( $= 100 \text{ kN/m}^2$ ), and
- $a$  = stress exponent ( $-1 \leq a \leq 1$ ).

A definition of the tangent modulus from the stress-strain behavior of the soil is shown in Figure 11. The same figure also shows the principal behavior of the tangent modulus for an overconsolidated clay. For the preconsolidated stress range, a constant modulus is indicated ( $a = 1$ ), whereas the modulus increases linearly ( $a = 0$ ) for stresses above the preconsolidation pressure  $\sigma_c'$ . The tangent modulus may be determined from a laboratory oedometer test.

In the CPTU interpretations, the vertical deformation moduli may be expressed as a function of the net cone resistance  $q_n$ . For clays, a linear interpretation model is suggested for the estimation of values of  $M$  for the preconsolidated stress range (Figure 11). The expression reads (19)

$$M_i = m_i \cdot q_n \quad (18)$$

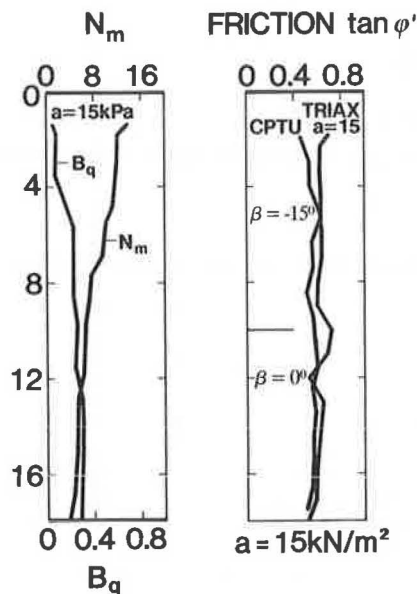


FIGURE 10 Comparison between in situ and laboratory values of  $\tan \phi'$  for Glava clay.

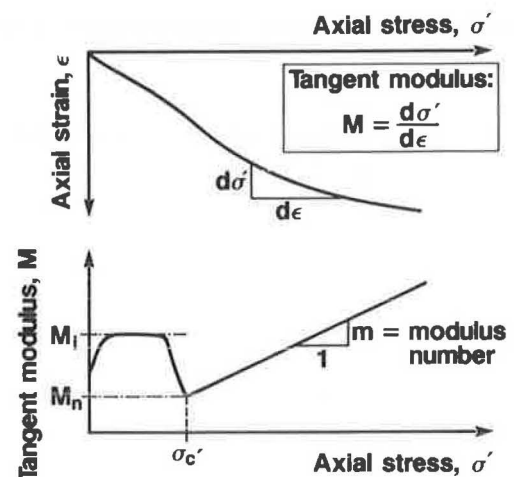


FIGURE 11 Definition of deformation moduli from CPTU.

The in situ modulus number  $m_i$  ranges from 5 to 15 in most clays (19). In the normally consolidated stress range, one may combine

$$M = m(\sigma'_{v0} + a) \quad (19)$$

and

$$q_n = N_m(\sigma'_{v0} + a) \quad (20)$$

and get

$$M_n = m_n \cdot q_n \quad (21)$$

where

$m_n$  = in situ modulus number ( $m/N_m$ ),  
 $m$  = oedometer modulus number, and  
 $N_m$  = cone resistance number.

Common values of  $m_n$  in clays may range from 4 to 8 (9). As shown in Figure 11,  $M_n$  corresponds to the oedometer modulus occurring at the preconsolidation pressure  $\sigma'_c$ .

In Figure 12, interpreted values of  $M_i$  are shown for Glava clay. Corresponding values of the oedometer modulus show good agreement with an average interpretation of  $10 \cdot q_n$ , and generally plot within the suggested range of  $\pm 5 \cdot q_n$ .

The modulus  $M_n$  at  $\sigma'_c$  is shown in Figure 13. Interpreted values compare well with the upper limit of  $8 \cdot q_n$ . The exam-

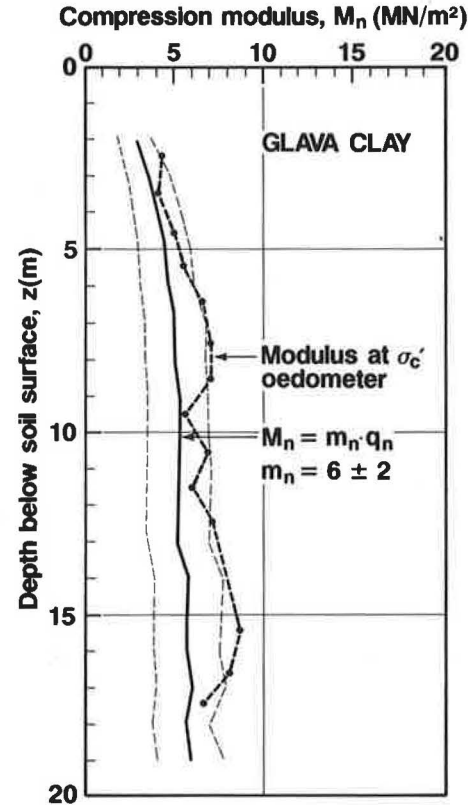


FIGURE 13 Compression modulus  $M_n$  for Glava clay.

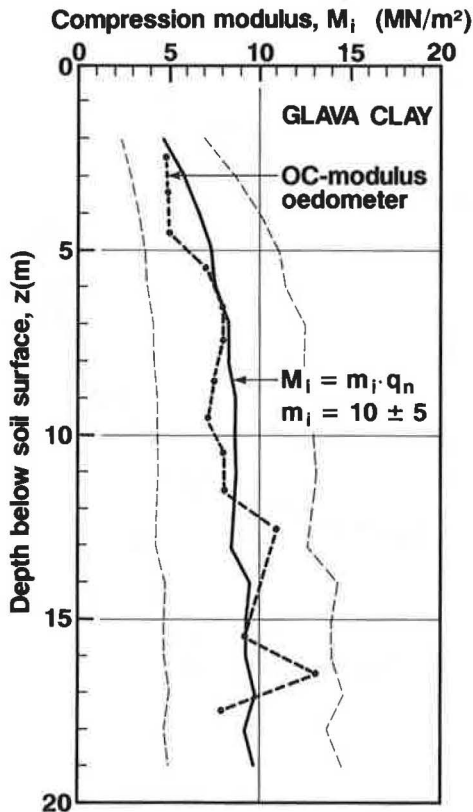


FIGURE 12 Compression modulus  $M_i$  for Glava clay.

ples indicate that, for clays, compression moduli may be fairly well predicted from simple, semiempirical relationships.

#### Stress History and Preconsolidation Pressure

Several methods have recently been presented for evaluation of the stress history of a soil on the basis of in situ tests (4). Such methods may give supplementary information besides the determination of the preconsolidation pressure from oedometer tests. A reliable interpretation of preconsolidation stress level is particularly important in soil types where it is difficult to obtain undisturbed, high-quality samples.

#### Cone Resistance in Preconsolidated Clays

It has previously been shown that the bearing capacity expression on total stress basis may be written as

$$q_T - \gamma z = N_c \cdot s_u \quad (22)$$

where

$N_c$  = bearing capacity factor,  
 $\gamma$  = unit weight of soil, and  
 $z$  = depth below soil surface.

For normally consolidated clays, the undrained shear strength may be expressed as:

$$s_u = \alpha_u \cdot (\gamma - \gamma_w) \cdot z = \alpha_u \cdot \gamma' \cdot z \quad (23)$$

By combining Equations 22 and 23, one obtains:

$$q_T = (N_c \cdot \alpha_u \cdot \gamma' / \gamma + 1) \cdot \gamma \cdot z = K_c \cdot \gamma \cdot z \quad (24)$$

where  $K_c$  is the cone resistance factor.

Typical values of  $\alpha_u$  range from 0.2 to 0.25, whereas  $N_c$  theoretically may vary between 6 and 10 in most bearing capacity approaches. The ratio  $\gamma' / \gamma$  lies approximately in the range from 0.5 to 0.6. The average value of  $K_c$  is hence close to 2.

Consequently, the theoretical cone resistance for a marine, homogeneous, normally consolidated clay may be written:

$$q_T \approx 2\bar{\gamma} \cdot z \quad (25)$$

where  $\bar{\gamma}$  is the average total unit weight of soil.

The stress history of a clay deposit may hence be evaluated by plotting a straight line  $2\bar{\gamma} \cdot z$  on the  $q_T - z$  record. If the  $q_T$  recordings plot is close to the theoretical line, the clay is most likely normally consolidated. If  $q_T$  is significantly larger than  $2\bar{\gamma} \cdot z$ , the clay may be in an overconsolidated state. Figure 14 shows this evaluation principle applied to CPTU records from overconsolidated Glava clay.

#### Approximation of Preconsolidation Pressure

When pore pressures are measured in a piezocone test, the in situ preconsolidation pressure  $\sigma'_c$  may be approximated from the expression published by Sandven et al. (9):

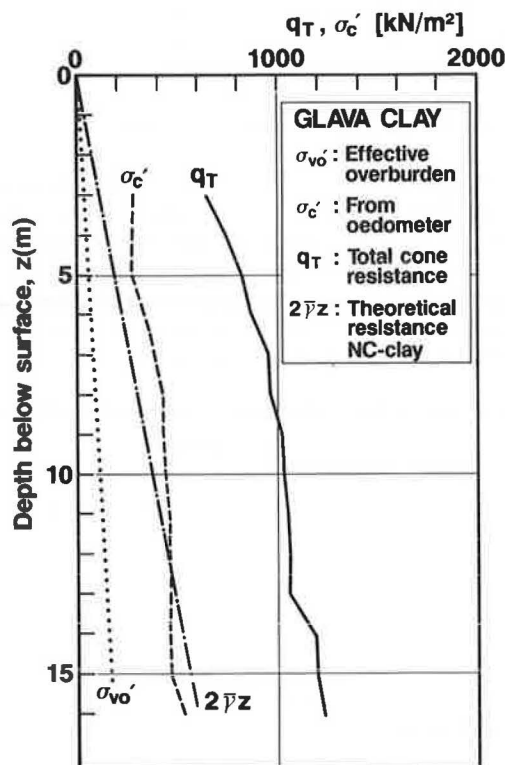


FIGURE 14 Cone resistance  $q_T$  versus preconsolidation pressure  $\sigma'_c$  for Glava clay.

$$\sigma'_c + a = \frac{q'_T + a}{N_{qc}} \quad (26)$$

where  $q'_T = q_T - u_T$  is the effective cone resistance, and  $N_{qc}$  is a bearing capacity coefficient defined by

$$N_{qc} = \frac{N_q + N_u B_q}{1 + N_u B_q} \quad (27)$$

The theoretical principles for this solution are similar to those applied for the interpretation of effective soil friction outlined in the section entitled "Soil Strength." In this approach, it is assumed that the effective cone resistance ( $q'_T$ ) depends on the preconsolidation stress ( $\sigma'_c$ ), the excess pore pressure around the cone ( $\Delta u_T$ ), and the effective shear strength parameters  $a$  and  $\tan \phi'$ . These factors are expressed in the bearing capacity coefficient  $N_{qc}$ , shown in Figure 15. The hatched area in the diagram reflects the variation in the product  $N_u B_q$  when the Prandtl solution for  $N_q$  ( $\beta = 0$  degrees) is used. The basis for the diagram is presently the subject of further research; hence the diagram may be modified when more data become available. Interpreted preconsolidation pressures from CPTU data for Glava clay are compared to corresponding values determined from oedometer tests in Figure 16. Some discrepancies are seen between the two values, especially below a depth of 10 m. However, continued research and further correlations in other clay types may improve the agreement between in situ and laboratory parameters.

#### Coefficient of Consolidation

When performing cone penetration tests in slow-draining soils, excess pore pressures will be generated in the surrounding soil. If the continuous cone penetration is stopped, this excess

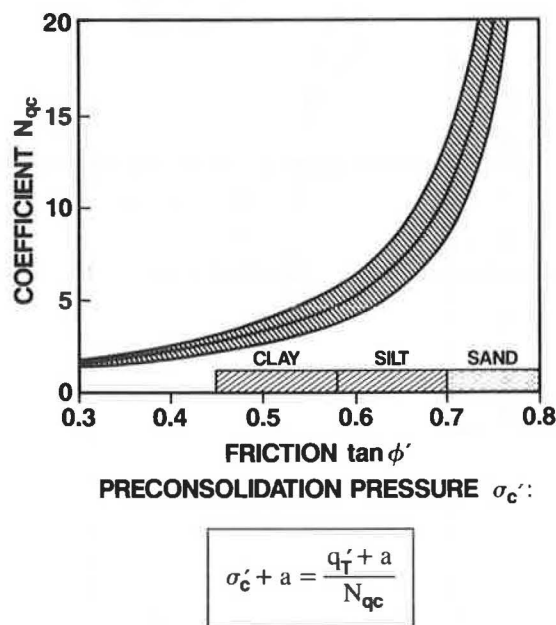


FIGURE 15 Bearing capacity coefficient  $N_{qc}$  for interpretation of preconsolidation pressure  $\sigma'_c$ .

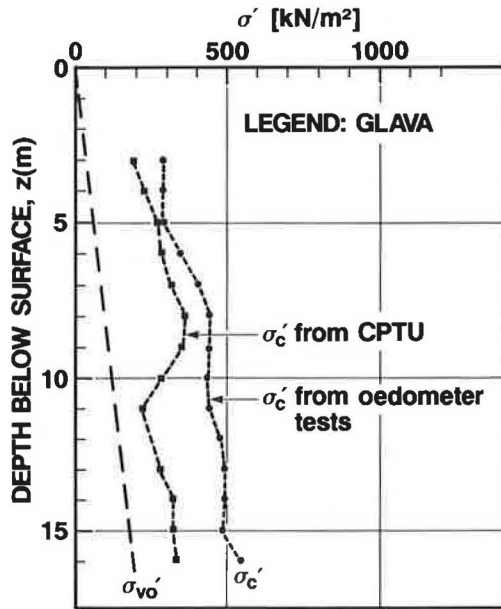


FIGURE 16 In situ and laboratory values of the preconsolidation pressure  $\sigma'_c$  for Glava clay.

pore pressure will start to dissipate, and the decay of pore pressure with time can be monitored.

#### Theoretical Considerations

Cone indentation in soils may be modelled by the expansion of a cylindrical or spherical cavity in an elastic, perfectly plastic medium (13,14). The cavity expansion is characterized by the development of a spherical or cylindrical plastic zone ( $\tau_f = s_u$ ) near the cone. Outside this zone, the soil is in a state of elastic equilibrium ( $\tau_f < s_u$ ). The extension of the plastified zone depends on the rigidity index of the soil ( $I_r = G/s_u$ , where  $G$  is the shear modulus of the soil). Several models based on cavity expansion theory have been developed in

order to interpret the coefficient of consolidation ( $c$ ) from dissipation test results (23). This parameter may be defined as follows:

$$c = \frac{M \cdot k}{\gamma_w} \quad (28)$$

where

$M$  = deformation modulus,  
 $k$  = soil permeability, and  
 $\gamma_w$  = unit weight of water.

Vertical ( $c_v$ ) and radial ( $c_r$ ) values of the coefficient of consolidation are usually somewhat different in natural soil deposits. At NTH, two different approaches are used to interpret dissipation test data (19). Both approaches are based on cylindrical cavity expansion theory, and should hence yield values for the radial coefficient of consolidation. Using the time-factor approach,

$$c_r = r_0^2 \cdot \frac{T}{t} \quad (29)$$

where

$r_0$  = probe diameter,  
 $T$  = time factor, and  
 $t$  = time to reach given level of dissipation.

Using the rate-factor approach,

$$c_r = r_0^2 \cdot \lambda_c \cdot \left| \frac{\Delta \dot{u}_T}{\Delta u_T} \right| \quad (30)$$

where

$\lambda_c$  = rate factor,  
 $\Delta \dot{u}_T$  = rate of pore pressure dissipation at given dissipation level, and  
 $\Delta u_T$  = initial excess pore pressure at  $t = 0$ .

A principal graph of test recordings and terminology is given in Figure 17, and values for the rate factor  $\lambda_c$  and time factor

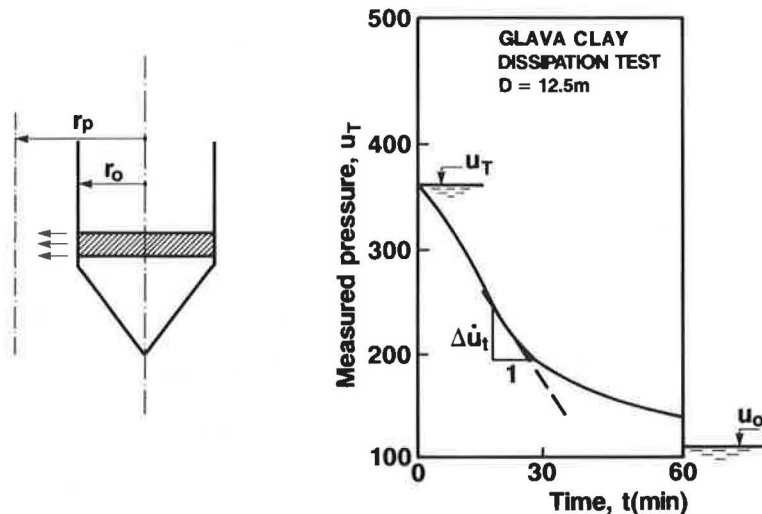


FIGURE 17 Principal graph and terminology for interpretation of CPTU dissipation tests.

$T$  are shown in Figures 18 and 19, respectively. Both factors depend on soil properties (rigidity index  $I_r$ ) and degree of dissipation ( $U_T$ ), where  $U_T$  (in percent) may be written as

$$U_T = \frac{\Delta u_t}{\Delta u_T} = \left| \frac{u_t - u_0}{u_T - u_0} \right| \cdot 100 \quad (31)$$

where

$u_t$  = pore pressure at given time  $t$ ,  
 $u_T$  = initial pore pressure at  $t = 0$ , and  
 $u_0$  = initial in situ pore pressure before penetration.

The coefficient of consolidation may vary with the effective stress level. It is, however, usually evaluated at a 50-percent degree of dissipation.

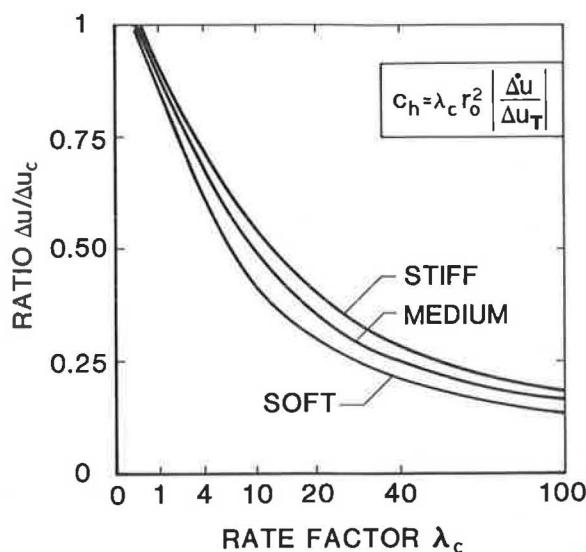


FIGURE 18 Diagram for interpretation of rate factor  $\lambda_c$ .

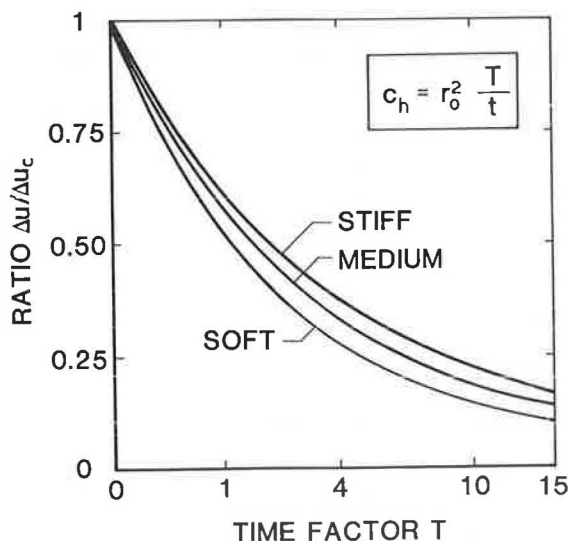


FIGURE 19 Diagram for interpretation of time factor  $T$ .

Several factors may complicate a successful interpretation of dissipation test data. For example (24),

- The dissipation curves are very sensitive to the initial distribution of the excess pore pressure in the plastic zone;
- Consolidation may take place in both vertical and horizontal directions;
- Soil behavior near the cone is complex, due to remolding during penetration, soil anisotropy effects, and soil macrostructure and stratification; and
- A rigid and sufficiently saturated pore pressure measuring system is necessary to give high-quality, reliable test results.

However, it seems that one-dimensional models based on cavity expansion theory may provide reasonably reliable predictions of the coefficient of consolidation. Interpreted values may correspond to values in the preconsolidated stress range in a laboratory test sample, at least for dissipation levels below 50 percent. This is because parts of the consolidation process will take place with the soil in an overconsolidated state. If a value of the coefficient of consolidation in the normally consolidated (NC) stress range is wanted, one may hence wait past the 50-percent level of dissipation.

### Results

Dissipation tests were carried out at five different levels in Glava clay. A piezocone with the filter located at the cylindrical part was used for the test, and hence it was assumed that the dissipation mainly takes place in the radial direction. Continuous consolidation tests were performed on undisturbed samples from the same level in the profile. These tests were performed on both vertically and horizontally oriented samples to evaluate the consolidation properties in both directions. In situ and laboratory values of the coefficient of consolidation are compared in Figure 20. In general, values predicted by the interpretation models are of the same order of magnitude as those determined on horizontal samples in the oedometer tests.

In the interpretations, the coefficient of consolidation has been evaluated at 50-percent pore pressure dissipation, and for medium-stiff soil conditions ( $I_r = 45$ ). The laboratory values have been selected as the average from the preconsolidated stress range. In this clay, the radial coefficient of consolidation was slightly greater than the vertical.

### CONCLUSIONS

Piezocone tests are a very promising method of obtaining realistic values of strength and deformation parameters in many soil types. The piezocone is also an excellent tool for the determination of soil stratification and the identification of soil type. Its potential for obtaining estimates of engineering soil parameters, along with its excellent determination of soil layering, has established the piezocone test as one of the outstanding and most promising methods of in situ investigation.

The test is today the dominant in situ method for offshore



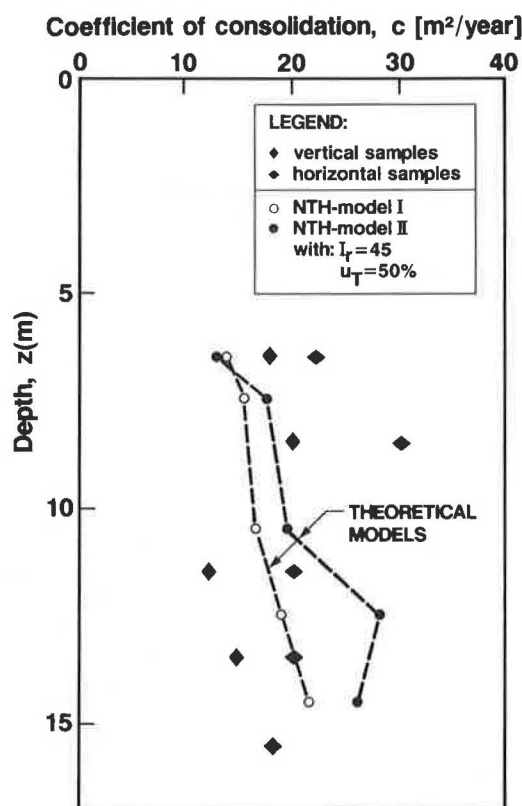


FIGURE 20 Comparison of in situ and laboratory values for the coefficient of consolidation ( $c$ ).

site investigations on the Norwegian Continental Shelf. It is particularly useful in deposits where it may be difficult to obtain undisturbed soil samples for onshore laboratory investigations. Research carried out in many countries and institutions further illustrates the potential of the test. It is reasonable to believe that new and improved interpretation models will emerge from this research and thus further improve the quality of the interpreted parameters.

## REFERENCES

1. N. Janbu and K. Senneset. Effective Stress Interpretation of In Situ Static Cone Penetration Tests. *Proc., 1st European Symposium on Penetration Testing, ESOPT I*, Stockholm, Sweden, Vol. 2.2, 1974, pp. 181–195.
2. B. A. Torstensson. Pore Pressure Sounding Instrument. *Proc., Conference on In Situ Measurement of Soil Properties*, Raleigh, N.C., Vol. 1, 1975, pp. 48–54.
3. A. E. Z. Wissa, R. T. Martin, and I. E. Garlenger. The Piezometer Probe. *Proc., Conference on In Situ Measurement of Soil Properties*, Raleigh, N.C., Vol. 1, 1975, pp. 536–545.
4. R. Campanella, P. K. Robertson, and D. Gillespie. Cone Penetration Testing in Deltaic Soils. *Canadian Geotechnical Journal*, Vol. 20, No. 1, 1983, pp. 23–35.
5. J. M. Konrad. Piezo-Friction-Cone Penetrometer Testing in Soft Clays. *Canadian Geotechnical Journal*, Vol. 24, 1987, pp. 645–652.
6. Technical Committee on Penetration Testing, International Society for Soil Mechanics and Foundation Engineering. International Reference Test Procedure. Proposal to International Society for Soil Mechanics and Foundation Engineering, Orlando, Florida, 1988.
7. T. Lunne, H. P. Christoffersen, and T. I. Tjelta. Engineering Use of Piezocone Data in North Sea Clays. *Proc., 11th International Conference on Soil Mechanics and Foundation Engineering*, San Francisco, Calif., 1985.
8. R. Campanella and P. K. Robertson. Current Status of the Piezocone Test. *Proc., 1st International Symposium on Penetration Testing, ISOPT-1*, Orlando, Fla., Vol. 1, 1988, pp. 93–116.
9. R. Sandven, K. Senneset, and N. Janbu. Interpretation of Piezocone Tests in Cohesive Soils. *Proc., 1st International Symposium on Penetration Testing, ISOPT-1*, Orlando, Fla., Vol. 2, 1988, pp. 939–955.
10. J. M. Konrad and K. T. Law. Undrained Shear Strength from Piezocone Tests. *Canadian Geotechnical Journal*, Vol. 14, 1987, pp. 392–405.
11. G. G. Meyerhof. The Ultimate Bearing Capacity of Wedge-Shaped Foundations. *Proc., 4th International Conference on Soil Mechanics and Foundation Engineering*, London, England, 1957, pp. 105–109.
12. K. Terzaghi. *Theoretical Soil Mechanics*. John Wiley & Sons, New York, 1943.
13. R. Hill. *The Mathematical Theory of Plasticity*. Oxford University Press, Oxford, England, 1950.
14. A. S. Vesic. Expansion of Cavities in Infinite Soil Mass. *Journal of the Soil Mechanics and Foundation Engineering Division, ASCE*, Vol. 98, No. SM3, 1972, pp. 265–290.
15. M. M. Baligh. Strain Path Method. *Journal of Geotechnical Engineering*, Vol. 111, No. 9, 1985, pp. 1108–1136.
16. G. Houlby and C. I. Teh. Analysis of the Piezocone in Clay. *Proc., 1st International Symposium on Penetration Testing, ESOPT-1*, Orlando, Fla., Vol. 2, 1988, pp. 777–783.
17. T. Lunne and A. Kleven. Role of CPT in North Sea Foundation Engineering. In *Cone Penetration Testing and Experience* (G. M. Norris et al., eds.), ASCE, New York, 1981, pp. 49–75.
18. K. Senneset and N. Janbu. Shear Strength Parameters Obtained from Static Cone Penetration Tests. In *Strength Testing of Marine Sediments*, ASTM STP 883, Philadelphia, Pa., 1985, pp. 41–54.
19. K. Senneset, N. Janbu, and G. Svanø. Strength and Deformation Parameters from Cone Penetration Tests. *Proc., 2nd European Symposium on Penetration Testing, ESOPT II*, Amsterdam, The Netherlands, Vol. 2, 1982, pp. 863–870.
20. S. Kirkebø. *Re-evaluation of the Bearing Capacity Factors  $N_q$ ,  $N_\gamma$ , and  $N_c$* . Diploma thesis. Geotechnical Division, Norwegian Institute of Technology, 1986.
21. K. Eggereide. Program Documentation for DATCPT (in Norwegian). O. Kummeneje A/S, Report No. 0.5024.3, 1985.
22. N. Janbu. Soil Compressibility as Determined by Oedometer and Triaxial Tests. *Proc., 3rd European Conference on Soil Mechanics and Foundation Engineering*, Wiesbaden, Germany, Vol. 1, 1963, pp. 19–25.
23. B. A. Torstensson. The Pore Pressure Probe. *Proc., NGF, Geoteknikdagen, Oslo*, 1977, pp. 34.1–34.15.
24. J. N. Levadoux and M. M. Baligh. Consolidation after Undrained Piezocone Penetration: I, Prediction. *Journal of Geotechnical Engineering*, Vol. 112, No. 7, 1986, pp. 707–726.

Publication of this paper sponsored by Committee on Soil and Rock Properties.